Analyst

ROYAL SOCIETY OF CHEMISTRY

PAPER

View Article Online
View Journal | View Issue

Cite this: *Analyst*, 2022, **147**, 2980

Smartphone-based autofluorescence imaging to detect bacterial species on laboratory surfaces†

Bailey C. Buchanan,‡ Babak Safavinia,‡ Lillian Wu and Jeong-Yeol Yoon *

The potential of bacterial contamination is commonly seen in biological and clinical laboratory surfaces, creating a need to detect the presence of bacteria on a surface. Various bacterial species have been found to naturally exist on surfaces, including *Escherichia coli*, *Salmonella* Typhimurium, and *Staphylococcus aureus* that were investigated in this study. Bacterial presence was identified from laboratory surfaces using a smartphone and low-cost components without culturing or staining. Autofluorescence from bacteria was quantified using a 405 nm LED as an excitation light source. A low-cost acrylic film could isolate the autofluorescence emission. ImageJ was used to process and analyze the images and quantify the emitted autofluorescence signal. This imaging platform successfully detected the presence of all three bacterial species from the heavily used laboratory surfaces. A trend of decreasing fluorescence signal was observed with decreasing bacterial concentration, and the limit of detection was 10^4 CFU cm^{-2}. It could also distinguish from tap water, protein (bovine serum albumin), and NaCl solutions. This preliminary work emphasizes the ability to detect autofluorescence signals of bacteria and non-microbial surface contaminants using a cost-effective and straightforward imaging platform.

Received 1st March 2022,
Accepted 24th May 2022

DOI: 10.1039/d2an00358a

rsc.li/analyst

Introduction

Bacterial species are commonly used or found in biological and clinical laboratory settings, leading to the potential of bacterial contamination. Laboratory experiments and clinical diagnoses may be influenced by bacterial contamination, which would lead to erroneous measurements and inaccurate results.[1] Therefore, there is a need to detect bacterial presence on laboratory and clinical surfaces.

Bacterial contamination can stem from various bacterial species that have been found to commonly exist on surfaces, including *Escherichia coli*, *Salmonella enterica* (including serovar Typhimurium), and *Staphylococcus* aureus.[2,3] It has been reported that *S. aureus* can survive well on many different surfaces.[2,4] In addition, *E. coli* was found to be one of the top five bacterial species on an anatomical model in a laboratory setting[3] and exhibiting strong attachment to abiotic surfaces.[5] All of these indicate that several bacterial species can survive on surfaces in a laboratory environment. Therefore, a rapid and low-cost bacterial detection method is needed to ensure that a laboratory surface is free of bacterial contamination.

Bacteria on laboratory surfaces have traditionally been identified and quantified by swabbing the surface, dissolving into a solution, and culturing them on selective or differential media.[6] Colonies are counted visually to quantify their amounts. While this method is low-cost and straightforward, it requires an overnight culture to see the results. Nucleic acid amplification techniques, most notably polymerase chain reaction (PCR), have also been popularly used, reducing the assay time to several hours. However, it requires specialized equipment such as a thermal cycler and a gel electrophoresis system (alternatively a real-time thermal cycler) and highly trained personnel to extract the gene and operate such equipment.[7] Antibody-based biosensors, typically incorporated on paper strips or microfluidic devices, have also popularly been investigated for bacterial detection.[8] However, they still require swab-sampling and manual loading onto the platforms. All of the above methods require sampling, manual sampling loading, and material preparations (media, PCR kits, antibodies, *etc.*). If we can detect the bacterial presence directly from the surface with neither sampling nor staining, it will provide a rapid and straightforward bacterial detection method from laboratory surfaces. In addition, it will be beneficial if we can also use a smartphone (specifically a smartphone camera) as an optical reader device, which has been widely investigated for numerous biosensing and medical diagnostics applications.[9]

This work aims to detect autofluorescence from bacteria using a smartphone camera and low-cost components (a light-emitting diode and an acrylic film) towards low-cost and

Department of Biomedical Engineering, The University of Arizona, Tucson, Arizona 85721, USA. E-mail: jyyoon@arizona.edu

† Electronic supplementary information (ESI) available. See DOI: **https://doi.org/10.1039/d2an00358a**

‡ These authors contributed equally.

straightforward bacteria detection from laboratory surfaces. Intrinsic fluorescence (autofluorescence) can be generated from bacterial species' cellular constituents, such as tryptophan in proteins, nucleic acids, lipofuscins, and especially porphyrins.[10,11] Such autofluorescence allows for the detection of bacteria without fluorescence staining.[12–15]

In this study, a bacterial autofluorescence imaging setup was created to detect surface-level bacterial contaminants. A smartphone platform was used to image a laboratory surface, utilizing the smartphone's advantages of being cost-effective and easy to image.[16,17] A single 405 nm light-emitting diode (LED) was used as a fluorescence excitation light source, and an acrylic film was used as a low-cost optical bandpass filter. A 405 nm LED was chosen due to its ability to excite bacterial species.[18–20] More specifically, porphyrins produced by bacteria are commonly used as a fluorescent biomarker that gets optimally excited by the 405 nm LED.[10,21,22] This 405 nm excitation should be specific to bacteria but not to tryptophan in proteins and nicotinamide adenine dinucleotide (NAD) (all excited by deep UV from 260–280 nm).[23] Indeed, the 405 nm excitation generated fluorescence emissions from all three bacterial species, while it did not induce significant autofluorescence from other fluorescing controls, including tap water, salt solution, and protein solution. This study aimed to create a smartphone platform that can detect bacterial species without fluorescence staining. This imaging setup can potentially be applied in the future to scan surfaces and identify bacterial presence on that surface. This practice can then limit the bacterial contamination found on the surfaces in laboratory and clinical settings.

Materials and methods

Bacteria culture

Three bacteria species were examined, including *Escherichia coli* K12 lyophilized powder (Sigma, St Louis, MO, USA), *Salmonella enterica* serovar Typhimurium Z005 strain (ZeptoMetrix, Buffalo, NY, USA), and methicillin-susceptible *Staphylococcus aureus* (MSSA, ZeptoMetrix, Buffalo, NY, USA). *E. coli* was cultured by first adding 10 mL of lysogeny broth (LB) to a 15 mL centrifuge tube. Next, a small scoop of about 1 μg of *E. coli* powder was added to the LB and mixed. The centrifuge tube was loosely sealed and then parafilmed on the cap. This tube was incubated for 24 h at 37 °C. The same procedure was completed to culture *S.* Typhimurium and *S. aureus*.

The concentration of each species was validated using a spectrophotometer, through measuring the optical density (OD) value at 600 nm from the miniature spectrophotometer (USB4000; Ocean Optics; Dunedin, FL, USA). The stock solution contained mostly LB and the bacterial density was determined to be approximately 10^8 CFU mL^{-1}. Serial dilutions were made to obtain bacterial concentrations of 10^7 CFU mL^{-1}, 10^6 CFU mL^{-1}, 10^5 CFU mL^{-1}, and 10^4 CFU mL^{-1}, using DI water. The intensity value of a blank cuvette of 1 mL of DI water was measured as a control, since the serial dilutions were made with DI water. While LB should be consumed during bacterial culture, small amount of LB should still be present in each dilution, *e.g.*, 10% LB in 10^7 CFU mL^{-1}, 1% in 10^6 CFU mL^{-1}, 0.1% in 10^5 CFU mL^{-1}, and 0.01% in 10^4 CFU mL^{-1}. There should be no residual LB in the experiments without LB, which is the main focus of this research.

A 10 μL drop was placed onto a surface (microscope slide or laboratory desk), and then the placed droplet was measured to be about 1 cm^2. A conversion was made to determine the surface concentration (CFU cm^{-2}) from the volumetric concentration (CFU mL^{-1}). Since 10 μL created 1 cm^2 surface, 10^8 CFU mL^{-1} became equivalent to 10^6 CFU cm^{-2}.

Imaging procedure

Acrylic film (#389; Color Filter Booklet; Edmund Optics, AZ, USA) was used as a low-cost optical bandpass filter, allowing only the wavelengths from 480 to 520 nm to pass through. The acrylic film was placed in front of the smartphone camera. The specific acrylic film was chosen after trial and error to be the optimal filter for isolating the autofluorescence signal. A smartphone camera (Samsung Galaxy S20 FE 5G; Samsung Electronics America, Inc., NJ, USA) was used to image bacterial droplets on surfaces. Any surface that was used to image was thoroughly cleaned with ethanol directly prior to imaging, to ensure that there were not any outside sources contributing to the autofluorescence signals. In order to simulate a real-life bacterial contamination, the droplets were placed on microscope slides or laboratory desks, and left to dry for 1–1.5 hours, after all the solvents were evaporated. The "pro" mode of the smartphone camera was used in taking images which allowed for the manual control: white balance = 2300 K, ISO = 200, shutter speed = 2 s. The smartphone was placed 10 cm above the droplets, perpendicularly. Initially, the use of the smartphone flashlight and another bandpass filter was proposed but was not chosen due to a low signal intensity at 405 nm. A 9 V battery was used to power the 405 nm LED, which was held 20 cm away from the droplets to minimize light reflectance (Fig. 1). The optimal distances of the smartphone and the LED from the droplet were chosen by the process of trial and error to ensure the images obtained were not under- or over-saturated.

Each bacteria species was diluted 10-fold three times to obtain concentrations of each species from 10^7 CFU mL^{-1} to 10^4 CFU mL^{-1}, or the equivalent surface level concentrations of 10^5 to 10^3 CFU cm^{-2}. These were the final concentrations used for imaging. For laboratory desk experiments, a black laboratory desk surface was cleaned with ethanol right before each imaging session. Then, six 20 μL droplets of each bacteria dilutions were placed onto the clean desk surface and allowed to dry for approximately 1–1.5 h, depending on when the droplets become fully dry. After the droplets were dry, images were taken by a smartphone with the acrylic film and the 405 nm LED irradiating from the side (Fig. 1).

We also used a commercial UV flashlight (Vansky UV Flashlight; purchased from Amazon) for comparison purposes. It contained 51 LEDs with the peak emission at 395 nm according to the manufacturer. While it is designed to detect

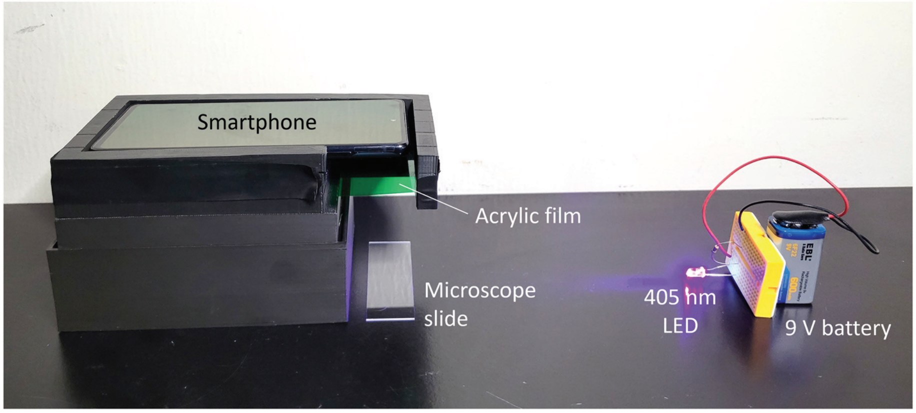

Fig. 1 Bacteria autofluorescence imaging set up on a laboratory desk. Acrylic film (as a low-cost optical bandpass filter) is placed in front of the Samsung S20 camera to isolate the autofluorescence signal. A 405 nm LED is used to excite the bacteria droplet from the side. 10 µL bacterial droplets are added on a microscope slide (shown in the figure) or directly on a laboratory desk surface.

pet urine and bugs, it may also induce autofluorescence to bacteria, although the manufacturer did not advertise such capability. An identical imaging procedure was used. The removal of the acrylic film ensures the duplication of the intended usage of this UV flashlight, since this device would typically be used to detect stains to the naked eye. Due to the high intensity of the UV flashlight, it was placed 50 cm away from the droplets, and images were taken.

Experiments without LB

While LB has been used to culture bacterial samples, LB may not be found in practical samples. In addition, it is known that LB itself exhibits autofluorescence, albeit not intensely. Therefore, after completing the experiments with the LB-cultured bacteria samples on microscope slides, additional experiments were performed with the bacteria samples whose LB was removed. 500 µL of each bacteria species in the growth media was removed and placed into a clear 2 mL centrifuge tube. Each species was spun in the microcentrifuge (Galaxy 16D; VWR, Radnor, PA, USA) at 6000 rpm for 8 min. The supernatant of each tube was removed, around 495 µL, and then the same amount (495 µL) of DI water was added and used to resuspend each bacteria pellet. The concentration of each species was then determined using the same steps as described previously.

Image analysis

ImageJ (US National Institutes of Health; Bethesda, MD, USA) was used to process and analyze the images taken by the smartphone. Images were first cropped to isolate the droplet and then were split into blue, green, and red channels. Since the expected autofluorescence was in the green wavelength range, only the green channel was used to analyze the images, as shown in Fig. 2. ImageJ generated the pixel intensities (ranging from 0 to 255; 8-bit) for all pixels, and provided the number of pixels (x_i) at specific pixel intensity (i), *e.g.*, 20 pixels showing the intensity of 100, 30 pixels showing the intensity of 101, *etc*. The following equation calculated the average intensity, where the denominator represents the total number of pixels, and the numerator represents all pixel intensities summed up. As shown in the equation, pixel intensities < 10 were not counted.

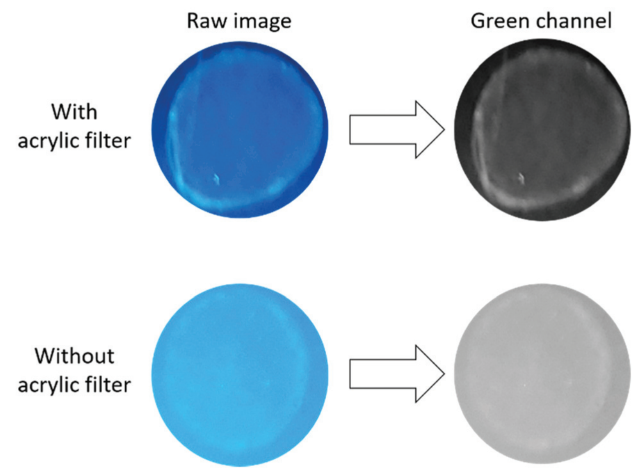

Fig. 2 Smartphone images (raw and green channel) of the bacteria droplets with *vs.* without an acrylic filter. Clearer fluorescence can be observed with an acrylic filter.

$$\text{Average intensity} = \frac{\sum_{i=10}^{255} (i \times x_i)}{\sum_{i=10}^{255} x_i}$$

Results and discussion

Bacteria species with LB imaged on microscope slides

Three different species of bacteria in LB were used for this experiment: *E. coli*, *S.* Typhimurium, and *S. aureus*. Each species was diluted from 10^6 CFU cm^{-2} (stock concentration) to 10^3 CFU cm^{-2}, and 6 droplets of each bacterial species at each concentration were placed on a microscope slide. The average intensity of each droplet was plotted against bacterial concentrations, as shown in Fig. 3. A diluted LB was the negative control for this experiment; LB was diluted in DI water. A linear decreasing trend was observed for the Gram-positive bacteria, *S. aureus*, whereas the Gram-negative bacteria, *E. coli* and *S.* Typhimurium, showed exponential decay. Nonetheless, all the bacterial species had a greater average intensity than the negative control, and it was confirmed that the autofluorescence was due to the presence of bacteria. The limit of detection (LOD) was 10^3 CFU cm^{-2}. Lower concentrations (not shown here) did not show significant differences from NC.

When the bacteria solution is diluted with DI water, the droplets form a ring-shaped structure (Fig. 3 on the top) due to the hydrophobicity of bacteria. The bacteria move towards the droplet's edges (three-phase borderline or contact line) to minimize their interactions with water molecules. Bacterial adhesion to hydrophobic surfaces has previously been demonstrated,[24] to minimize the entropy penalty provided by water molecules. At the three-phase borderline, the interaction with water molecules is minimized, where the bacteria are adsorbed to and pinned. Prior research has shown that *E. coli* and *S.* Typhimurium are more hydrophobic than *S. aureus*.[25,26] Greater hydrophobicity of *E. coli* and *S.* Typhimurium can be attributed to their Gram-negative cell walls compared to Gram-positive *S. aureus*.[27] While Gram-positive cell walls are characterized by one thick peptidoglycan wall, Gram-negative cell walls possess an additional second outer membrane made of particularly hydrophobic lipopolysaccharides. This explains the steeper exponential decay in *E. coli* and *S.* Typhimurium average intensities. High-level accumulation of such hydrophobic bacteria at the droplet's edges upon dilution would greatly diminish the intensity from the overall droplet. Although *S. aureus* is also hydrophobic, the fluorescence signal is more spread out upon dilution, causing a more linear decrease in average intensity.

Bacteria species with LB imaged on laboratory desks

Bacterial droplets were placed on a laboratory desk to represent a practical laboratory spillage. Similar trends were observed, and the LOD was again 10^3 CFU cm^{-2} (Fig. 4). A black laboratory desk was chosen as it is standard in most laboratories. It also decreased the light reflection that might influence the average intensity. Microscope slide (glass) and laboratory desk (wood) are both hydrophilic surfaces, which causes the diluted bacteria to spread more with low contact angles, which is ideal for autofluorescence imaging. Bacterial concentrations did not significantly vary the droplet sizes. Since there was an overlap between the negative control and 10^3 CFU cm^{-2} bacteria, in the next set of experiments, LB was removed from the solution to eliminate fluorescent signals from LB.

Selection of controls

One of the main goals of this work was to observe surface contaminants in a laboratory environment. Therefore, several solutions that could be found in a laboratory setting were chosen as controls. Tap water was selected as it is commonly found on laboratory surfaces, typically around the sink area. Salt solution was chosen as another control due to its possibility of being commonly found on a laboratory surface. In addition, proteins, specifically bovine serum albumin (BSA) that are commonly used in biological laboratories, would offer an

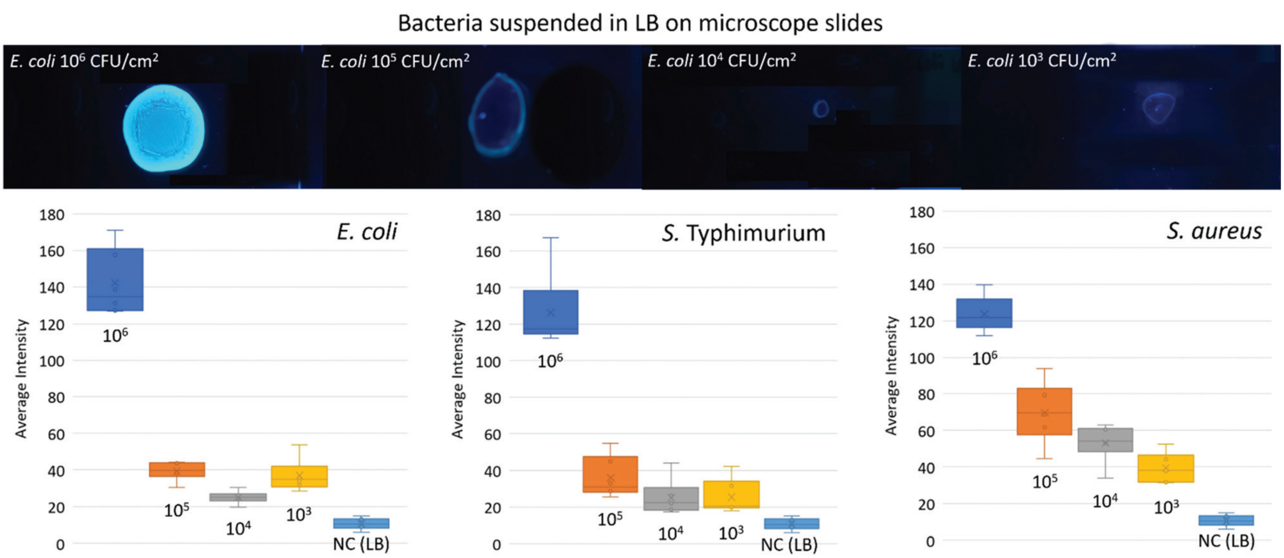

Fig. 3 Box and whisker plots of average intensities for bacteria droplets (suspended in LB and diluted in DI water) placed on microscope slides. Example images of *E. coli* droplets at various concentrations are shown in the top. Bottom shows the box and whisker plots of *E. coli*, *S.* Typhimurium, and *S. aureus* droplets at various concentrations (all in CFU cm^{-2}). Negative control (NC) on each plot is a dilution of three orders of magnitude of LB.

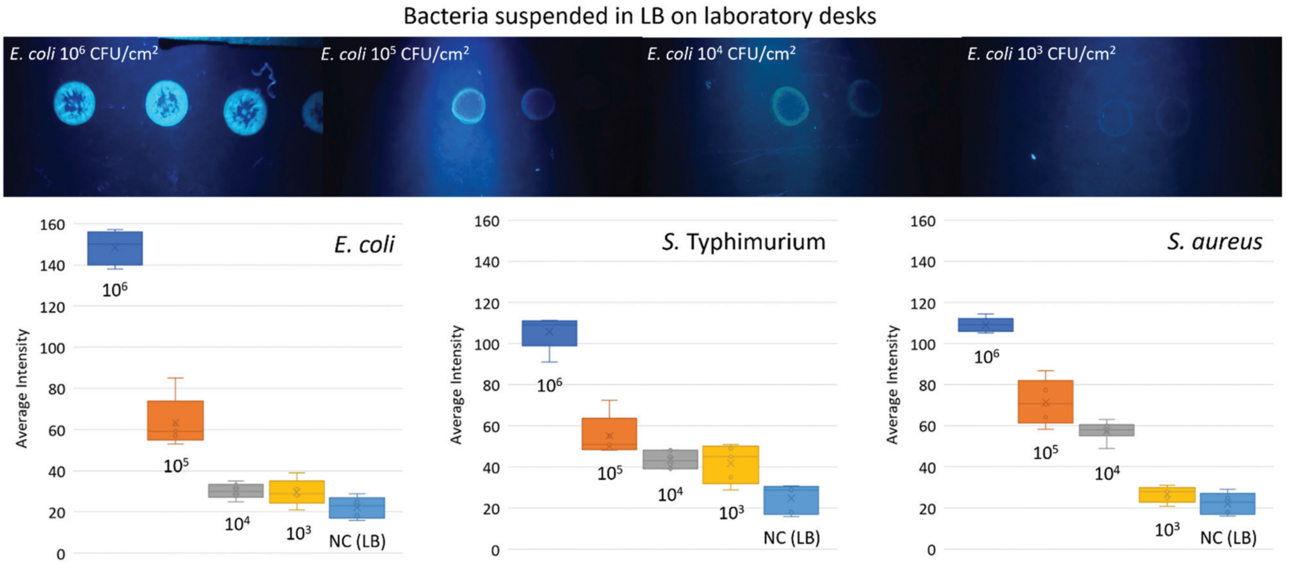

Fig. 4 Box and whisker plots of average intensities for bacteria droplets (suspended in LB and diluted in DI water) placed on laboratory desks. Example images of *E. coli* droplets at various concentrations are shown in the top. Bottom shows the box and whisker plots of *E. coli*, *S.* Typhimurium, and *S. aureus* droplets at various concentrations (all in CFU cm^{-2}). Negative control (NC) on each plot is a dilution of three orders of magnitude of LB.

excellent comparison to bacteria. BSA also emits fluorescence signals at 550 nm when excited with a 380 nm light source.[26] The autofluorescence of BSA can be attributed to its two tryptophan residues: Trp-134 and Trp-212 – both demonstrate intrinsic fluorescence.[28] Finally, since each bacteria species was suspended in LB or resuspended in DI water, both were also used as controls depending on the experiments.

Bacteria species resuspended in DI water imaged on laboratory desks

The same three species of bacteria, *E. coli*, *S.* Typhimurium, and *S. aureus*, were used in this set of experiments. The main difference in these experiments is the removal of LB from the bacteria samples. In the previous set of experiments, it was determined that some of the autofluorescence signals were coming from the presence of LB. Due to this, additional experiments were run to test the autofluorescence intensity of serially diluted LB (ESI Fig. 1†). Autofluorescence was observed for all serially diluted LBs with the expected decreasing trend.

To remove any interference from the culture media, LB was removed as described in the experiments without LB section to ensure no autofluorescence from LB. This removal ensured that none of the signals was coming from LB. In order to ensure that the resuspended bacteria were still alive, a 10^7 CFU mL^{-1} sample of each resuspended (in DI water) bacterial species were plated on a LB agar plate and left in the incubator overnight. As a control, a 10^7 CFU mL^{-1} concentration of each bacterial species suspended in LB were plated on a LB agar plate and incubated overnight as well. The colonies formed in both the control and the resuspended bacteria were similar, therefore the bacteria detected on the laboratory desk were still alive and the results in Fig. 5 were not affected. In

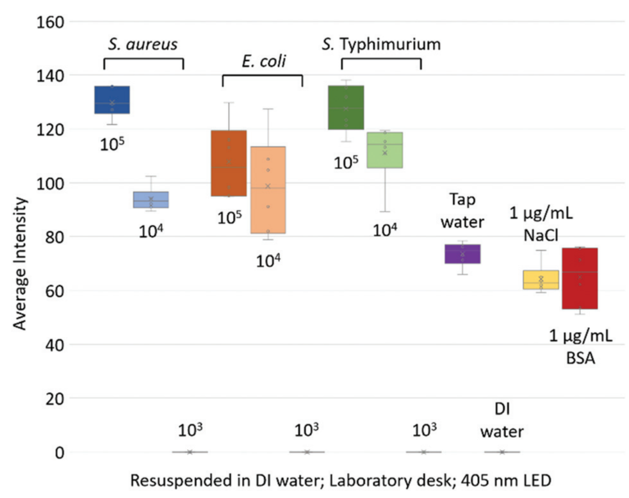

Fig. 5 Box and whisker plot of the average intensities of each bacteria species, *E. coli*, *S.* Typhimurium, and *S. aureus*, at the concentrations of 10^5, 10^4, and 10^3 CFU cm^{-2}. LB was removed from bacterial samples. A smartphone, a 405 nm LED, an acrylic film, and green channel images were used. The controls of tap water (0.8–1.2 ppm), DI water, NaCl solution (1 µg mL^{-1}), and BSA solution (1 µg mL^{-1}) are also plotted. These control concentrations are equivalent to 10 ng cm^{-2}, approximating the LOD of bacteria, 10^4 CFU cm^{-2}.

addition, various control samples were also tested, as explained in the previous section. Fig. 5 represents the average intensity values of each bacteria species, *E. coli*, *S.* Typhimurium, and *S. aureus*, at concentrations of 10^5, 10^4, and 10^3 CFU cm^{-2} for each species. In this set of experiments, 10^6 CFU cm^{-2} concentration was not tested since the LB removal decreased the stock concentration to 10^7 CFU mL^{-1} (=10^5 CFU cm^{-2}). The average intensity value of each bacteria species at 10^5 CFU cm^{-2} was higher than its counterpart at 10^4 CFU cm^{-2}. This decrease in the average autofluorescence intensity is analogous to the results shown in Fig. 4. Finally, images were taken for each bacterial species at 10^3 CFU cm^{-2}; however, no signal was detected (zero intensities). The intensity of DI water was also zero since there was no LB contributing to the autofluorescence. This leads the LOD to be 10^4 CFU cm^{-2}. The traditional method of swabbing a surface typically would have a LOD of 10^4 CFU mL^{-1}, which would be equivalent to 10^2 CFU cm^{-2} for a surface concentration.[29] Although a lower limit of detection would be more ideal, the observed LOD may be sufficient in identifying moderate-to-severe bacterial contaminations, in a low-cost, time effective, and simple manner. Besides, the method required neither swabbing nor culturing. Fig. 5 also includes the average intensity values of each of the controls. The controls of NaCl (model salt) and BSA (model protein) were made at 1 μg mL^{-1}, representing the surface concentration of 10 ng cm^{-2}. This concentration is equivalent to the LOD of 10^4 CFU cm^{-2}, since 1 CFU bacteria was approximated to be 1 pg. This conversion was made based on the standard dry mass of an *E. coli* cell, 1 pg, assuming that one cell will form 1 CFU.[30] Tap water was also used; according to the local water supplier, its chlorine level is regulated from 0.8 to 1.2 ppm (=0.8 to 1.2 μg mL^{-1}). Again, this chlorine concentration is equivalent to 8–12 mg cm^{-2}. The presence of chlorine in the tap water is hypothesized to create some autofluorescence signal, as previously demonstrated,[31] which can also be observed in Fig. 5 and 6. As mentioned earlier, BSA contains tryptophan that is responsible for the fluorescence signal observed in Fig. 5. However, 405 nm optimally excites porphyrins in bacteria but not tryptophan in BSA (optimally excited at 280 nm),[23] and hence the bacterial species emits a higher fluorescence signal. The average intensity for each control is lower than the average intensity values for the 10^5 CFU cm^{-2} and 10^4 CFU cm^{-2} concentrations. This result demonstrates a difference in the average autofluorescence intensities between bacterial species and non-microbial controls.

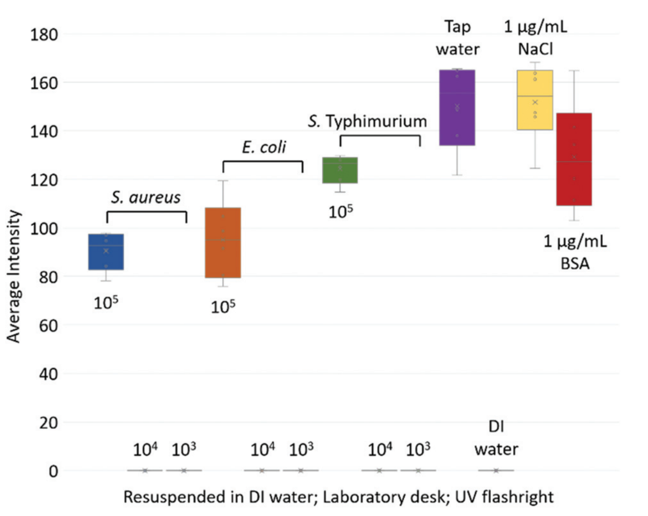

Fig. 6 Experiments were repeated with a commercial UV flashlight instead of a 405 nm LED. Blue channel images were used. All other conditions are identical to those shown in Fig. 5.

Experiments with a commercial UV flashlight

A UV flashlight was purchased and used to image each bacteria species, *E. coli, S.* Typhimurium, and *S. aureus*, from 10^5 through 10^3 CFU cm^{-2} and each of the controls mentioned in the previous section. Fig. 6 displays the average intensity values obtained for each bacteria species and controls. Since the excitation was UV at 395 nm, the blue channel was analyzed instead of the green channel.[32–34] In addition, the commercial UV flashlight provided a higher light intensity compared to the 405 nm LED. Therefore, the UV flashlight was placed further away from the droplets as described in materials and methods to prevent over-saturation in the fluorescence signal. The UV flashlight could not detect any of the bacteria species at a concentration of 10^4 CFU cm^{-2} and below, leading to the zero values that appear in Fig. 6. Although the wavelength of the flashlight was similar to our system's light source, it was not optimized for collecting the bacterial autofluorescence and the high number of LEDs in the flashlight and its distance from the droplet prevents it from exciting the droplet as precisely as the single 405 nm LED in our system. While the bacterial samples at 10^5 CFU cm^{-2} showed strong blue intensities, all three control samples – tap water, NaCl solution, and BSA solution – also showed strong blue signals, which rendered this method unable to identify bacterial presence on laboratory desk surfaces.

Conclusions

Bacteria contaminations in biological and clinical laboratory settings are common due to the nature of the research or hospital-wide microbial infection. However, there are no known methods to effectively detect bacteria on laboratory surfaces using autofluorescence signals. In this work, a smartphone platform was implemented to create an imaging setup that could image autofluorescence signals emitting from various bacteria species (*E. coli, S.* Typhimurium, and *S. aureus*) and controls (tap water, salt solution, and protein solution). Only a low-cost acrylic film and an LED were necessary, in addition to a smartphone. The images were processed through ImageJ to obtain average intensity values that could be compared against each other. When comparing bacteria species and controls using our imaging setup, the bacterial species exhibited an overall higher average intensity value than the controls test. The limit of detection was 10^4 CFU cm^{-2}. Whereas the UV flashlight was unable to differentiate between bacteria and controls, making our imaging setup a superior method. This preliminary work highlights the ability of cost-effective materials, such as a smartphone platform, a 405 nm LED, and an acrylic film, to image potential laboratory surface contaminants. Future work should include the development of a smartphone application that allows for analyzing images and detecting bacterial presence directly from the smartphone.

Author contributions

Bailey C. Buchanan: Conceptualization, data curation, formal analysis, investigation, methodology, resources, validation, visualization, writing – original draft. Babak Safavinia: Conceptualization, data curation, formal analysis, investigation, methodology, resources, validation, visualization, writing – original draft. Lillian Wu: Data curation, formal analysis, investigation. Jeong-Yeol Yoon: Conceptualization, formal analysis, funding acquisition, methodology, project administration, resources, supervision, validation, visualization, writing – review & editing.

Conflicts of interest

There are no conflicts to declare.

Acknowledgements

This work was supported by the University of Arizona's Test All Test Smart program and the Arizona Board of Regent's Technology and Research Initiative Fund (TRIF). We thank Dr Sangsik Kim for his help with bacteria culture.

References

1 E. Abatenh, B. Gizaw and Z. Tsegaye, Contamination in a microbiological laboratory, *Int. J. Res. Stud. Biosci.*, 2018, **6**, 7–13.
2 L. S. Y. Ng, W. T. Teh, S. K. Ng, L. C. Eng and T. Y. Tan, Bacterial contamination of hands and the environment in a microbiology laboratory, *J. Hosp. Infect.*, 2011, **78**, 231–233.
3 R. Kosif and F. Avcioglu, An examination of bacterial contamination of models used in anatomy laboratories, *Interdiscip. Perspect. Infect. Dis.*, 2018, **2018**, 9201312.
4 M. Schmidlin, M. Alt, G. Vogel, U. Voegeli, P. Brodmann and C. Bagutti, Contaminations of laboratory surfaces with Staphylococcus aureus are affected by the carrier status of laboratory staff, *J. Appl. Microbiol.*, 2010, **109**, 1284–1293.
5 R. M. Goulter, I. R. Gentle and G. A. Dykes, Issues in determining factors influencing bacterial attachment: A review using the attachment of Escherichia coli to abiotic surfaces as an example, *Lett. Appl. Microbiol.*, 2009, **49**, 1–7.
6 R. E. Sweeney, E. Budiman and J.-Y. Yoon, Mie scatter spectra-based device for instant, contact-free, and specific diagnosis of bacterial skin infection, *Sci. Rep.*, 2017, **7**, 4801.
7 S. V. Angus, S. Cho, D. K. Harshman, J.-Y. Song and J.-Y. Yoon, A portable, shock-proof, surface-heated droplet PCR system for Escherichia coli detection, *Biosens. Bioelectron.*, 2015, **74**, 360–368.
8 K. E. McCracken, S. V. Angus, K. A. Reynolds and J.-Y. Yoon, Multimodal imaging and lighting bias correction for improved μPAD-based water quality monitoring via smartphones, *Sci. Rep.*, 2016, **6**, 27529.
9 J.-Y. Yoon, *Smartphone Based Medical Diagnostics*, Elsevier, London/San Diego/Cambridge, 2020.
10 M. Y. Rennie, D. Dunham, L. Lindvere-Teene, R. Raizman, R. Hill and R. Linden, Understanding real-time fluorescence signals from bacteria and wound tissues observed with the MolecuLight i:X™, *Diagnostics*, 2019, **9**, 22.
11 J. Surre, C. Saint-Ruf, V. Collin, S. Orenga, M. Ramjeet and I. Matic, Strong increase in the autofluorescence of cells signals struggle for survival, *Sci. Rep.*, 2018, **8**, 12088.
12 L. Yang, Y. Zhou, S. Zhu, T. Huang, L. Wu and X. Yan, Detection and quantification of bacterial autofluorescence at the single-cell level by a laboratory-built high-sensitivity flow cytometer, *Anal. Chem.*, 2012, **84**, 1526–1532.
13 S. Patiño, L. Alamo, M. Cimino, Y. Casart, F. Bartoli, M. J. García and L. Salazar, Autofluorescence of mycobacteria as a tool for detection of Mycobacterium tuberculosis, *J. Clin. Microbiol.*, 2008, **46**, 3296–3302.
14 M. S. Ammor, Recent advances in the use of intrinsic fluorescence for bacterial identification and characterization, *J. Fluoresc.*, 2007, **17**, 455–459.
15 L. Leblanc and E. Dufour, Monitoring the identity of bacteria using their intrinsic fluorescence, *FEMS Microbiol. Lett.*, 2002, **211**, 147–153.
16 S. Gupta, A. Kumar, S. Thakur, A. Gupta, S. Vashisht and D. Singh, Cost effective DIY smartphone based retinal imaging, *2nd International Conference on Intelligent Engineering and Management*, 2021, pp. 471–475.
17 P. Kheampheta and P. Masawat, A simple and cost-effective smartphone-based digital imaging device for the quantification of selected heavy metals in Thai rice, *Anal. Method*, 2022, **14**, 165–173.
18 M. Y. Rennie, D. Dunham, L. Lindvere-Teene, R. Raizman, R. Hill and R. Linden, Understanding real-time fluorescence signals from bacteria and wound tissues observed with the MolecuLight, *Diagnostics*, 2019, **9**, 22.
19 S. Kang, E. de Josselin de Jong, S. M. Higham, C. K. Hope and B. Kim, Fluorescence fingerprints of oral bacteria, *J. Biophotonics*, 2020, **13**, e201900190.
20 J. S. Dickson and M. Koohmaraie, Cell surface charge characteristics and their relationship to bacterial attachment to meat surfaces, *Appl. Environ. Microbiol.*, 1989, **55**, 832–836.
21 M. Shu, S. Kuo, Y. Wang, Y. Jiang, Y. T. Liu, R. L. Gallo and C. M. Huang, Porphyrin metabolisms in human skin commensal Propionibacterium acnes bacteria: potential application to monitor human radiation risk, *Curr. Med. Chem.*, 2013, **20**, 562–568.
22 J. Fyrestam, N. Bjurshammar, E. Paulsson, A. Johannsen and C. Östman, Determination of porphyrins in oral bacteria by liquid chromatography electrospray ionization

tandem mass spectrometry, *Anal. Bioanal. Chem.*, 2015, **407**, 7013–7023.

23 A. B. Ghiasaidoobe and S. J. Chung, Intrinsic tryptophan fluorescence in the detection and analysis of proteins: a focus on Förster resonance energy transfer techniques, *Int. J. Mol. Sci.*, 2014, **15**, 22518–22538.

24 M. C. van Loosdrecht, J. Lyklema, W. Norde, G. Schraa and A. J. Zehnder, The role of bacterial cell wall hydrophobicity in adhesion, *Appl. Environ. Microbiol.*, 1987, **53**, 1893–1897.

25 S. Kim, A. Romero-Lozano, D. S. Hwang and J.-Y. Yoon, A guanidinium-rich polymer as a new universal bioreceptor for multiplex detection of bacteria from environmental samples, *J. Hazard. Mater.*, 2021, **413**, 125538.

26 X. Ma, X. Sun, D. Hargrove, J. Chen, D. Song, Q. Dong, X. Lu, T. Fan, Y. Fu and Y. Lei, A biocompatible and biodegradable protein hydrogel with green and red autofluorescence: Preparation, characterization and in vivo biodegradation tracking and modeling, *Sci. Rep.*, 2016, **6**, 19370.

27 A. Ebbensgaard, H. Mordhorst, F. M. Aarestrup and E. B. Hansen, The role of outer membrane proteins and lipopolysaccharides for the sensitivity of Escherichia coli to antimicrobial peptides, *Front. Microbiol.*, 2018, **9**, 2153.

28 M. Tan, W. Liang, X. Luo and Y. Gu, Fluorescence spectroscopy study on the interaction between Evodiamine and bovine serum albumin, *J. Chem.*, 2013, **2013**, 308054.

29 *C. Griffith*, Surface sampling and the detection of contamination, *Handbook of Hygiene Control in the Food Industry*, ed. H. Lelieveld, J. Holah and D. Gabric, 2nd edn, 2016, pp. 673–696.

30 A. C. Guo, T. Jewison, M. Wilson, Y. Liu, C. Knox, Y. Djoumbou, P. Lo, R. Mandal, R. Krishnamurthy and D. S. Wishart, ECMDB: The *E. coli* metabolome database, *Nucleic Acids Res.*, 2012, **41**, D625–D630.

31 S. Chung, L. E. Breshears, A. Gonzales, C. M. Jennings, C. M. Morrison, W. Q. Betancourt, K. A. Reynolds and J.-Y. Yoon, Norovirus detection in water samples at the level of single virus copies per microliter using a smartphone-based fluorescence microscope, *Nat. Protoc.*, 2021, **16**, 1452–1475.

32 J.-Y. Yoon, *Introduction to Biosensors: From Electric Circuits to Immunosensors*, Springer, New York, USA, 2nd edn, 2016, pp. 153–170.

33 K. Xiao, B. Han, J. Sun, J. Tan, J. Yu, S. Liang, Y. Shen and X. Huang, Stokes shift and specific fluorescence as potential indicators of organic matter hydrophobicity and molecular weight in membrane bioreactors, *Environ. Sci. Technol.*, 2019, **53**(15), 8985–8993.

34 H. R. Petty, V. M. Elner, T. Kawaji, A. Clark, D. Thompson and D. Yang, A facile method for immunofluorescence microscopy of highly autofluorescent human retinal sections using nanoparticles with large Stokes shifts, *J. Neurosci. Methods*, 2010, **191**, 222–226.

